

ALMA Memo #296

Fitting of the Largest Configuration (≥ 10 km) into the Terrain at the Chajnantor Site

L. Kogan¹

(1) - National Radio Astronomy Observatory, Socorro, New Mexico, USA

March 9, 2000

Abstract

The result of fitting the largest ALMA's configuration ($\geq 10km$) into the terrain at the Chajnantor site is presented. The two cases were considered:

The initial doughnut configuration is fitted to the terrain with the only topography constraint.

The initial doughnut configuration is fitted to the terrain with the both topography and the doughnut constraint.

The array configurations are optimized minimizing side lobes in the fitting process. The topography constraint prevents to close the initial symmetry configuration at the north-west direction. The beam shape and the side lobe level are shown for the two cases in comparison with the case of absence of the topography constraint. Both snapshot and 6hr tracks simulation have been considered.

1 Discussion

Two years ago the first fit of an array configuration ([2]) to the terrain at the Chajnantor site was carried out. The file of the terrain had been prepared by Mark Holdaway. The terrain was given at the area 6x7 km with the cell 40 meters. Recently Bryan Butler created the new file which describes wider area (19x18 km) with better resolution (10 meters). Two files with the limit slope of 10° and 5° are available now both in FITS and ASCII format. To handle the new much bigger files I made necessary modification of the AIPS task CONF1 which carries out optimization of an array configuration minimizing side lobes ([1]) with different constraint including topography.

John Conway ([5]) has fitted a spiral zoom array of 3km size using the area located south/west of the pipe line. The same area was used in the memo ([2]). To fit a circular array of $\sim 10km$ size I selected the area surrounding the circle mount touching the pipe line from the north/east side of the pipe.

At the beginning I carried out optimization of the 64 element array at the snapshot mode without a topography constraint with two doughnut constraints: wide doughnut-the inner circle radius is equal to 0.25 of the outer circle diameter; and narrow doughnut-the inner circle radius

is equal to 0.4 of the outer circle diameter. The side lobes of the optimized array were less than 5.5% for the wide doughnut and 13.5% for the narrow one. I used the narrow doughnut as an initial configuration for the fitting. The outer diameter of the doughnut is selected equal to 12 km. The fitting has been carried out with the topography constraint only and with the both topography and the doughnut constraint. At the first case the better result side lobes could be expected. But the shape of the configuration can be very different of the initial doughnut.

I used the Bryan's file with 10 degree local gradient. The result of the fitting for the two cases are shown at the figures 1 and 2. The arrays shown in the figures are centered at East-10880m, North-9370m relatively the bottom left corner of the mask.

Figures 3 and 4 show the configurations (diamonds) and UV coverage (dots) at the snapshot mode in the normalized scale. The large circle mountain at the north-west (center at 630km east, 7457km north) prevents to close the initial symmetry configuration. As a result the UV coverage and relevant beam have a small asymmetry.

To get the beam patterns of the arrays I used the AIPS task UVCON for simulating UV data. Having had the UV data the whole power of AIPS can be used for imaging, plotting, printing, editing. In particular the standard AIPS tasks UVPLT, IMAGR, KNTR, LWPLA were used for creating the UV coverage and beam pattern files in PS format.

2 Snapshot and 6 hour tracks simulation

Figures 5, 6, 7, 8 represent the beam patterns for the two arrays for the two areas at the sky for snapshot simulation. The large area (512x512) includes far side lobes and the small area (32x32) includes only nearest side lobes.

The comparison of side lobes is given at the table 1. As it was expected the topography constraint prevents reaching the side lobe level obtained without constraint ($\sim 5\%$). When the only topography constraint is used the side lobes achieved after the optimization (9.8 %) are reasonably good.

Table 1: Comparison of the side lobe level for the array with and without the topography constraint.

	Snapshot		6hr tracks	
	near side lobes %	far side lobes %	near side lobes %	far side lobes %
Wide doughnut (0.25)	5.5	5.5		
Narrow doughnut (0.4)	14	14		
Topography constraint only	9.8	10	8	< 2
Topography and narrow doughnut constraint	21	18	17	< 5

Figures 9, and 10 show the UV coverage of the two 6hr tracks configurations. The data were created each 100sec. The AIPS task UVPLT used to create the UV coverage files. To diminish the file's size I plot only each fifth visibility. So the actual UV coverage is more complete.

Figures 11, 12, 13, 14 represent the beam patterns for the two arrays for the two areas at the sky for the 6hr tracks simulation. The large area (512x512) includes far side lobes and

the small area (32x32) includes only nearest side lobes. Comparing the beams of the snapshot and the 6hr tracks simulation (table 1) we see a great suppression of the far side lobes at the 6hr tracks simulation. The change of the nearest side lobes is not so visible. This result can be predicted. Using rotation of the Earth to improve UV coverage we approach to the continuous aperture which should have decreasing of the side lobe levels with increasing the distance from the main lobe. The nearest side lobes are determined mostly by the behavior of the UV coverage at its edge. The more tapering of the UV coverage density is the lower near side lobes should be. Including rotation of the Earth does not improve usually the tapering.

3 Conclusion

The two large configuration ($\sim 12km$) are fitted to the terrain at the Chajnantor Site. The first one is limited by the narrow doughnut. The side lobes have been minimized at the fitting process. The mount at the north-west of the mask prevents the best parameters of the fitting array. Still the configuration which is not limited by the doughnut has rather good side lobes.

I used the side lobe metric to compare the array configurations. The two simulation carried out by J. Conway ([4]) for a spiral array and by L. Kogan ([3]) for the circular compact configuration show (at least comparing with a ring array) that the lower side lobes are the better the imaging performance is.

References

- [1] L.R. Kogan, MMA memo 171, Optimization of of an Array Configuration Minimizing Side Lobes. 1997
- [2] L.R. Kogan, MMA memo 202, Optimization of of an Array Configuration with a Topography Constraint. 1998
- [3] L.R. Kogan, MMA memo 247, The Imaging Characteristics of an Array with Minimum Side Lobes. I. 1999
- [4] J. Conway, MMA memo 291, First Simulations of Imaging Performance of a Spiral Zoom Array; Comparison with a Single Ring Array. 2000
- [5] J. Conway, MMA memo 292, A Possible Layout for a Spiral Zoom ARRAY Incorporating Terrain Constraints. 2000

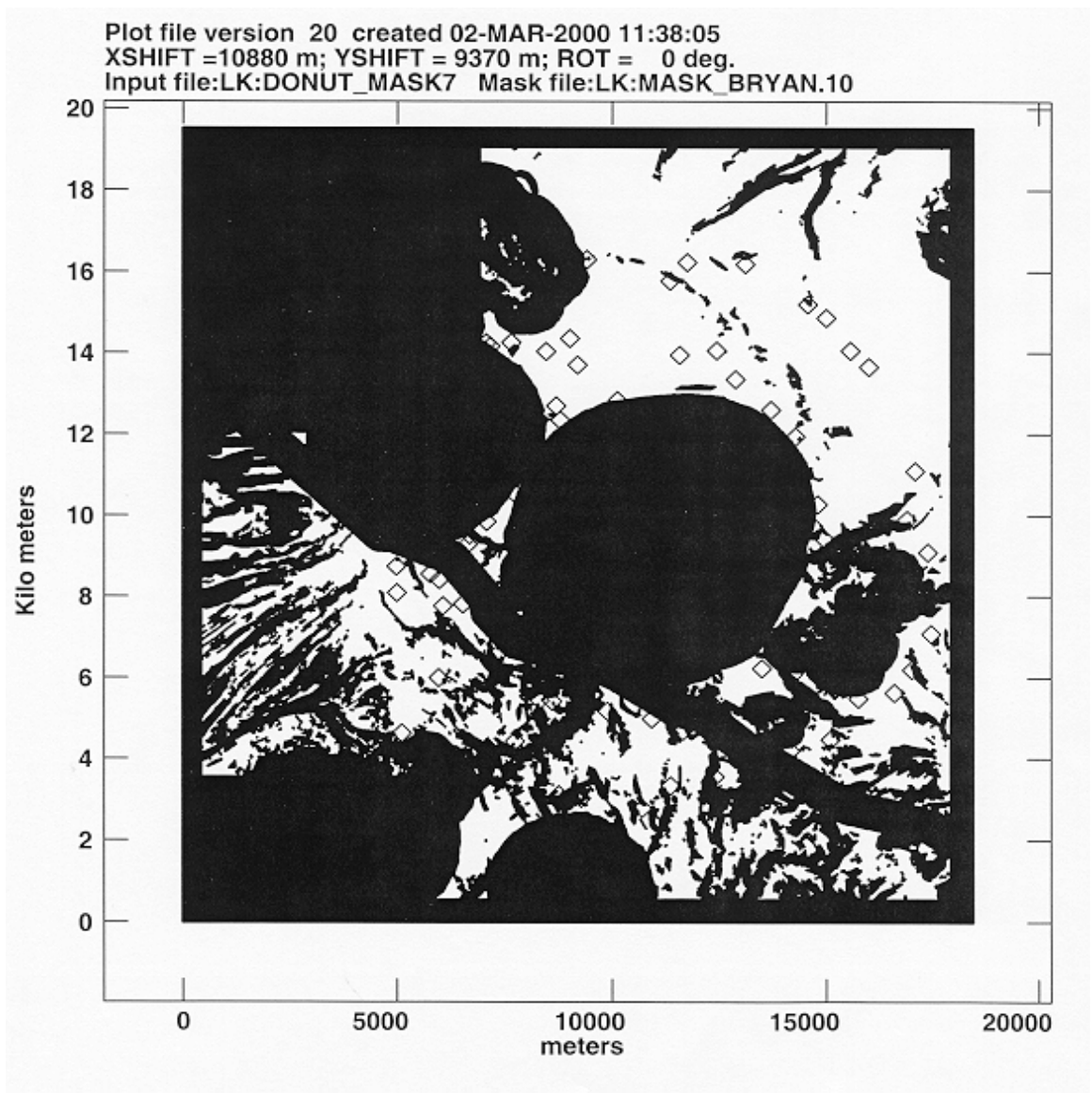


Figure 1: Array superimposed on 10 degree local gradient mask. The configuration is obtained optimizing side lobes with the topography as the only constraint.

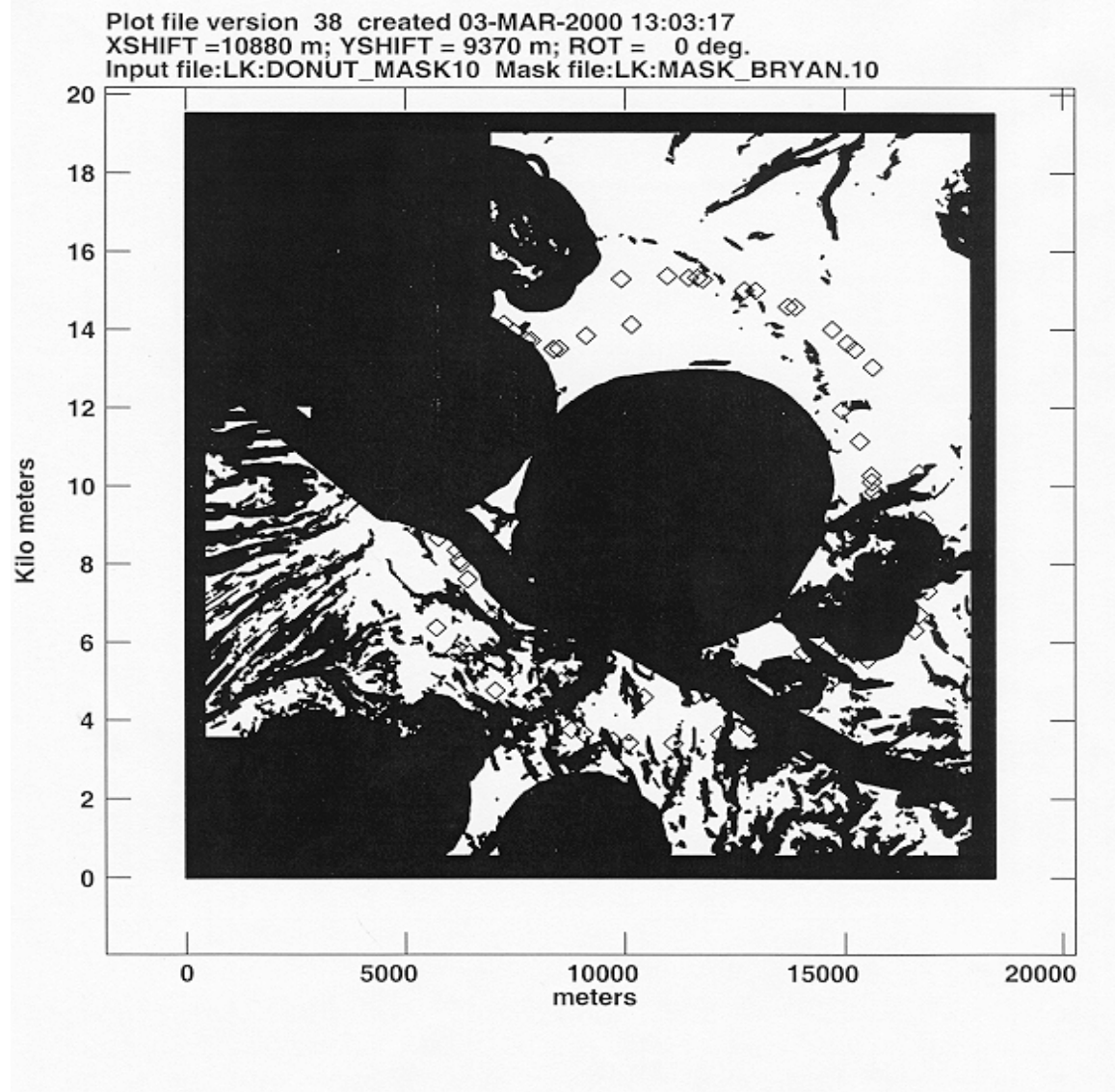


Figure 2: Array superimposed on 10 degree local gradient mask. The configuration is obtained optimizing side lobes with both the topography and the doughnut constraints.

Plot file version 22 created 02-MAR-2000 13:25:58
The worst sidelobe = 0.098; X = -11.8; Y = -9.4
Input file:LK:DONUT_MASK7 Iteration number 1. Elev = 90deg

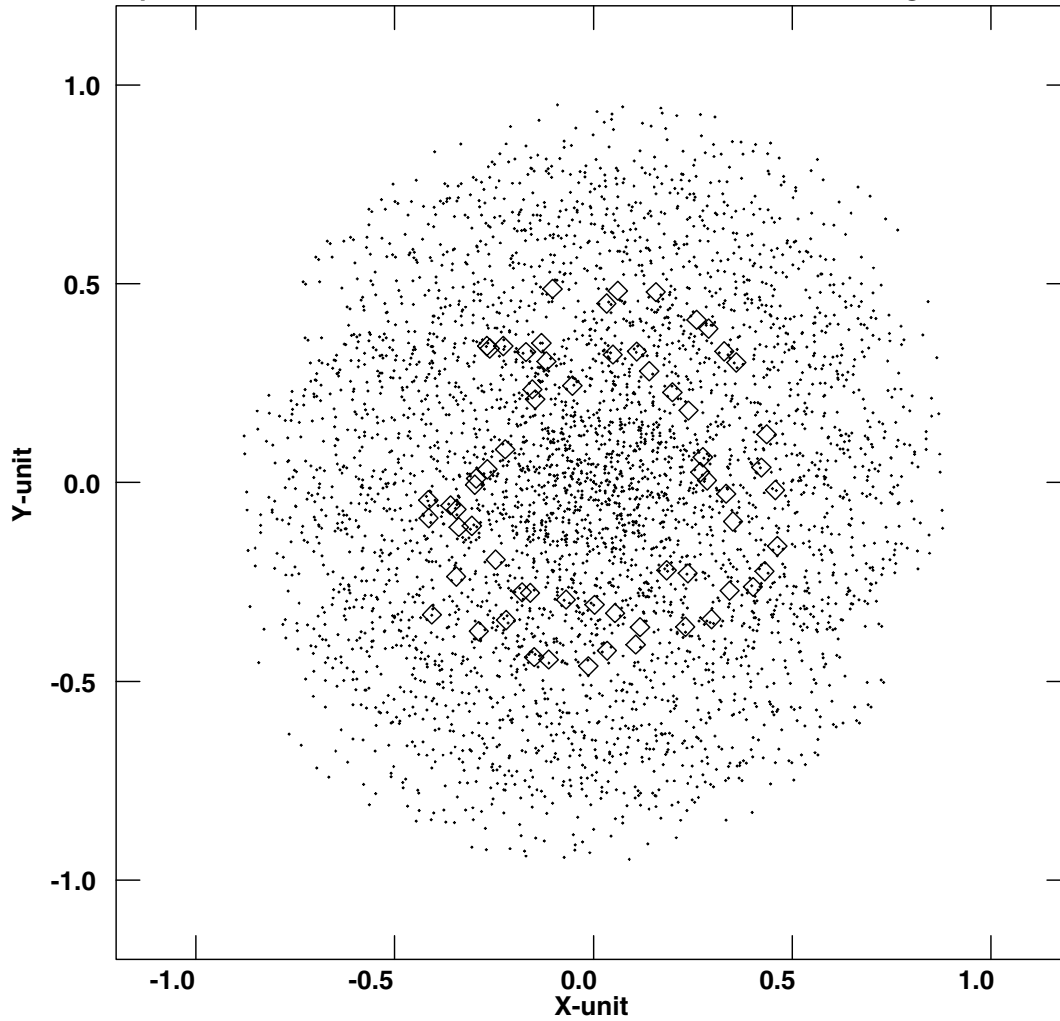


Figure 3: Configuration (diamonds) and snapshot UV coverage (dots) of the normalized array fitted to the terrain. The topography is the only constraint of the fitting/optimization. Size of the array is 12 kilometers.

Plot file version 40 created 03-MAR-2000 13:20:25
The worst sidelobe = 0.211; X = -0.6; Y = -1.2
Input file:LK:DONUT_MASK10 Iteration number 1. Elev = 90deg

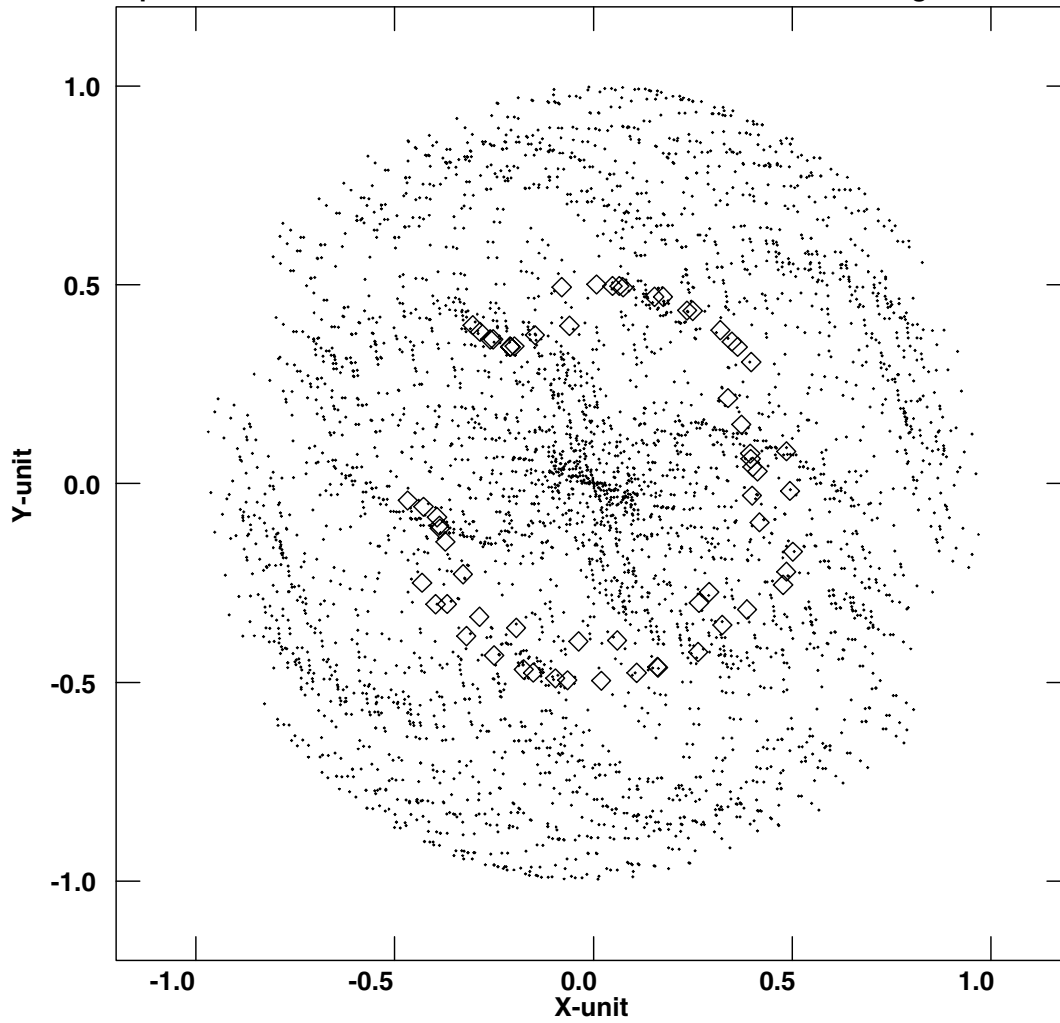


Figure 4: Configuration (diamonds) and snapshot UV coverage (dots) of the normalized array fitted to the terrain. The two constraints topography and doughnut were used at the fitting/optimization process. Size of the array is 12 kilometers.

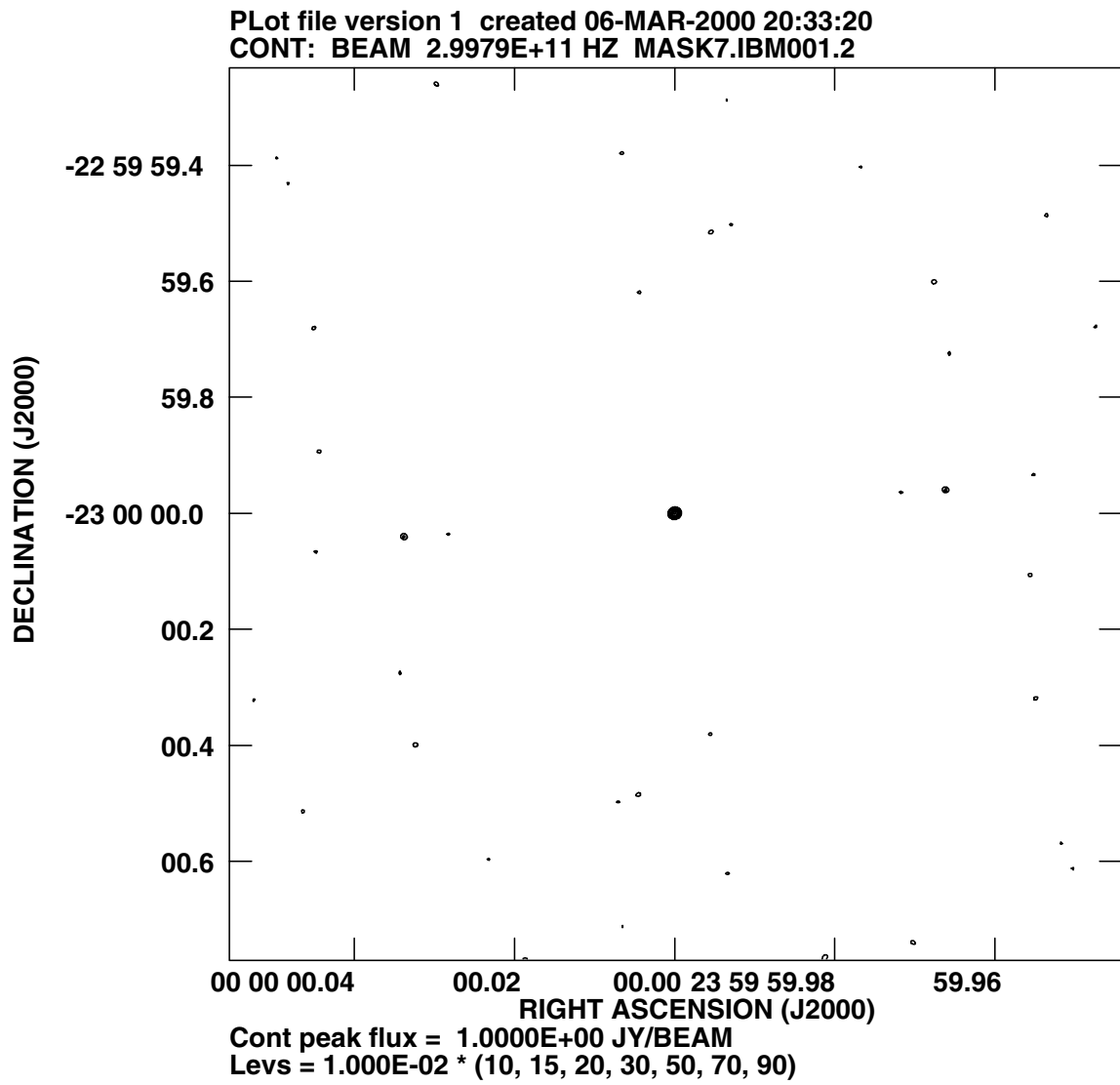


Figure 5: Snapshot observations. Beam pattern of the array fitted to the terrain using only topography constraints. The field (512×512 , cell = $0.2 \frac{\lambda}{D}$, $\lambda = 1mm$) includes far side lobes. The side lobe level is about 10 %.

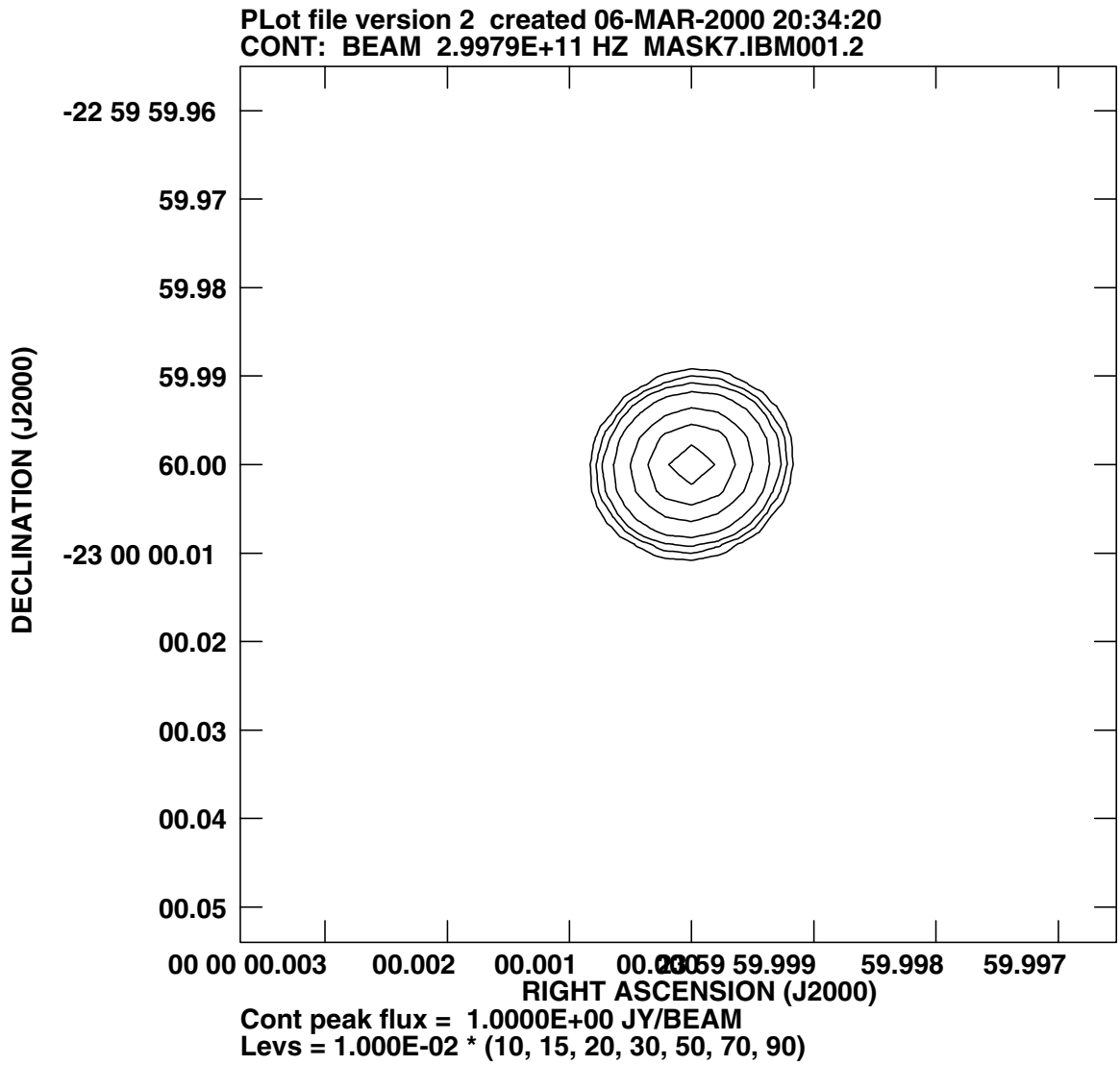


Figure 6: Snapshot observations. Beam pattern of the array fitted to the terrain using only topography constraints. The field (32×32 , cell = $0.2 \frac{\lambda}{D}$, $\lambda = 1mm$) includes only nearest side lobes. The side lobe level is about 10 %.

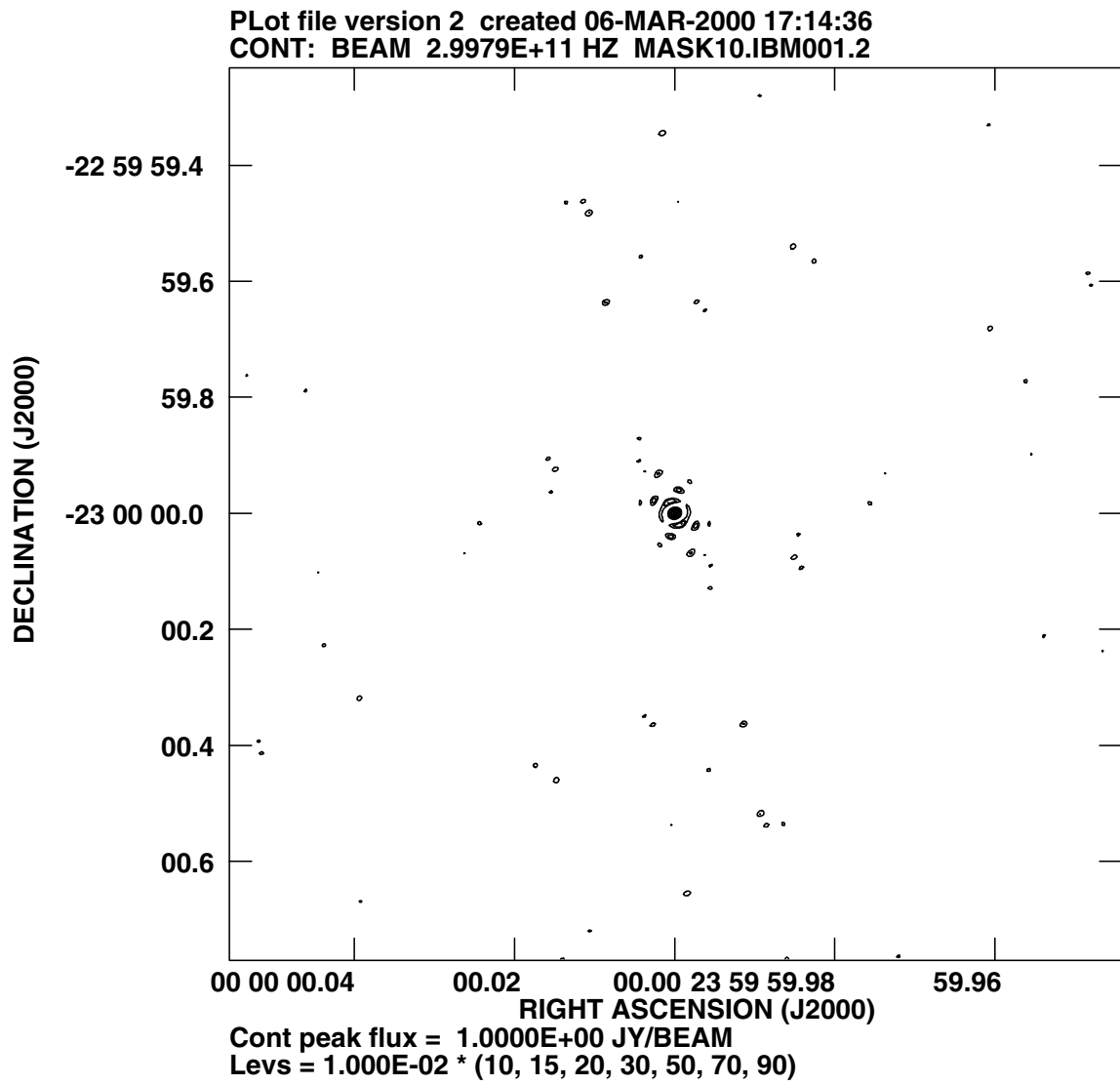


Figure 7: Snapshot observations. Beam pattern of the array fitted to the terrain using topography and doughnut constraints. The field (512×512 , cell = $0.2 \frac{\lambda}{D}$, $\lambda = 1mm$) includes far side lobes. The side lobe level is about 20 %.

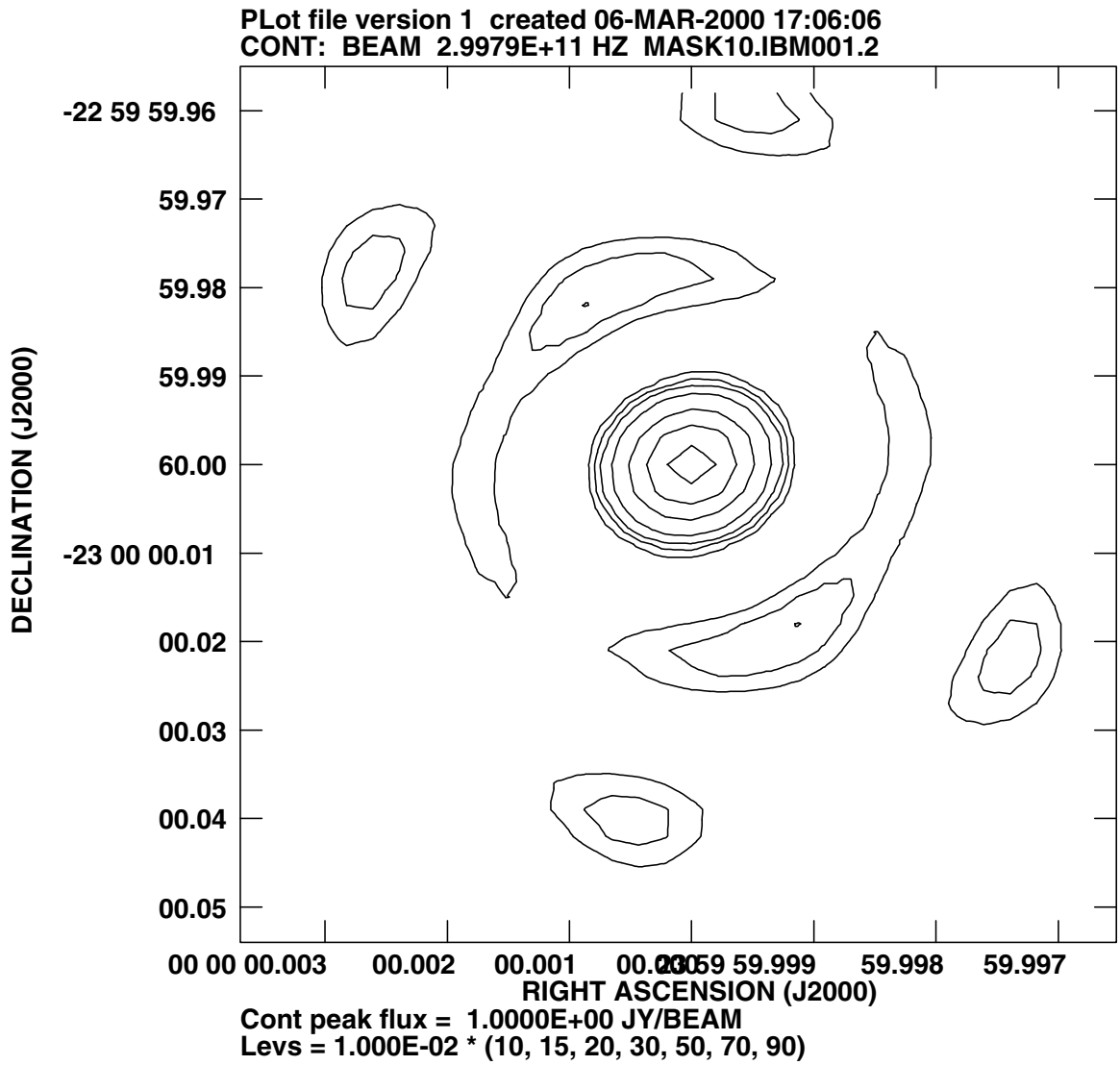


Figure 8: Snapshot observations. Beam pattern of the array fitted to the terrain using topography and doughnut constraints. The field (32×32 , cell = $0.2 \frac{\lambda}{D}$, $\lambda = 1mm$) includes only nearest side lobes. The side lobe level is about 20 %.

Plot file version 1 created 07-MAR-2000 09:46:37
V vs U for MASK7_6H.UVCON.1 Source:
Ants * - * Stokes I IF# 1 Chan# 1

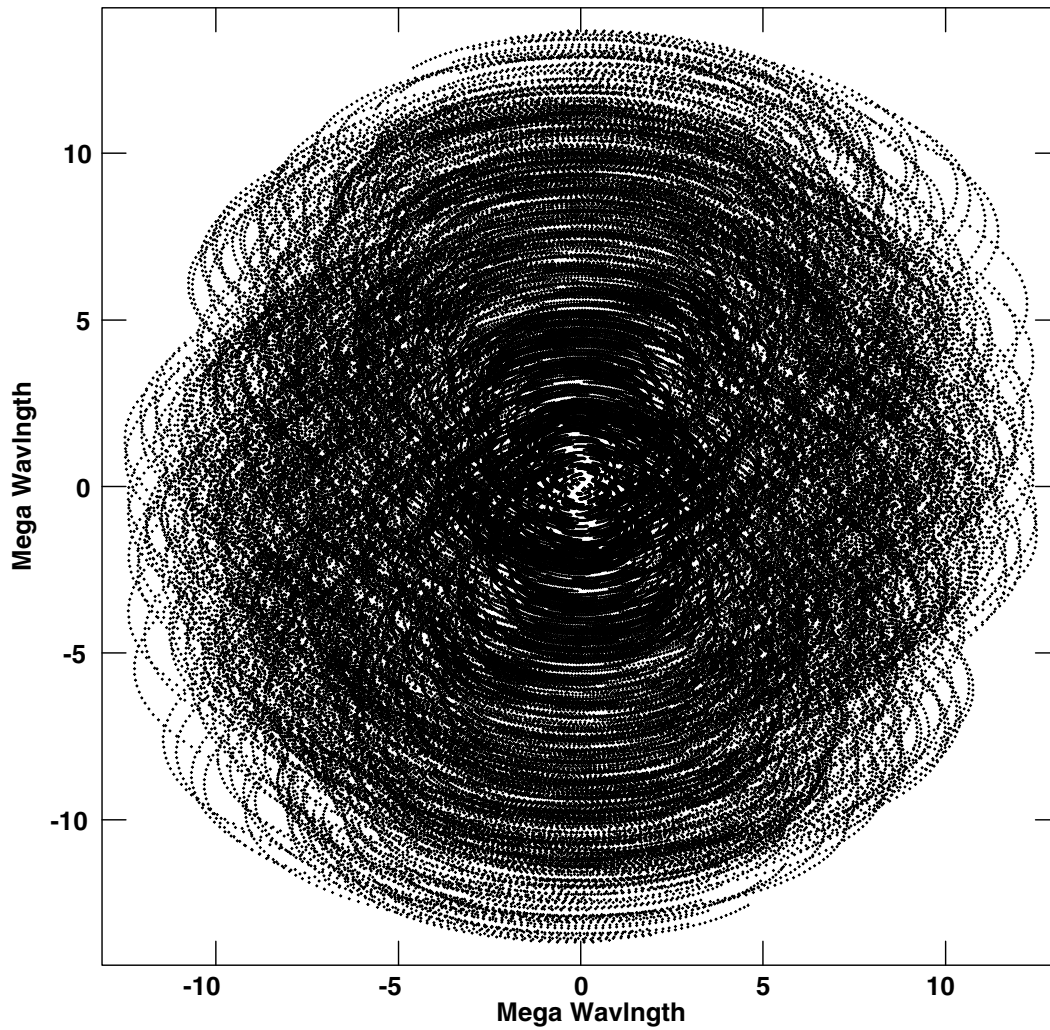


Figure 9: Six hour tracks observations. UV coverage of the array fitted to the terrain. The topography is the only constraint used at the fitting/optimization process. The AIPS task UVPLT used to create this file. Four visibilities of each five ones are skipped to diminish the size of the file. So actual UV coverage is more complete.

Plot file version 1 created 07-MAR-2000 09:27:55
V vs U for MASK10_6H.UVCON.1 Source:
Ants * - * Stokes I IF# 1 Chan# 1

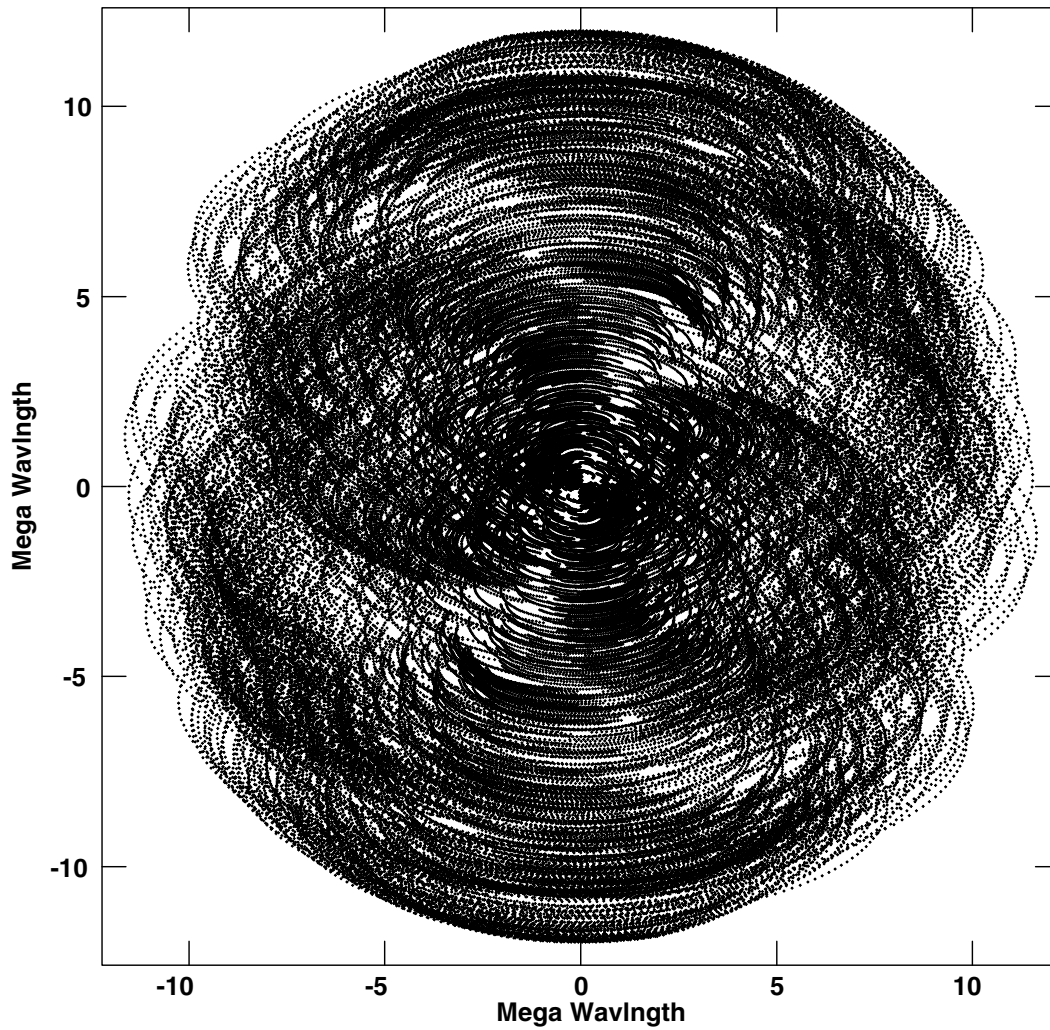


Figure 10: Six hour tracks observations. UV coverage of the array fitted to the terrain. The two constraints topography and doughnut were used at the fitting/optimization process. The AIPS task UVPLT used to create this file. Four visibilities of each five ones are skipped to diminish the size of the file. So actual UV coverage is more complete.

PLot file version 3 created 07-MAR-2000 10:42:31
CONT: BEAM 2.9979E+11 HZ MASK10 6H.IBM001.1

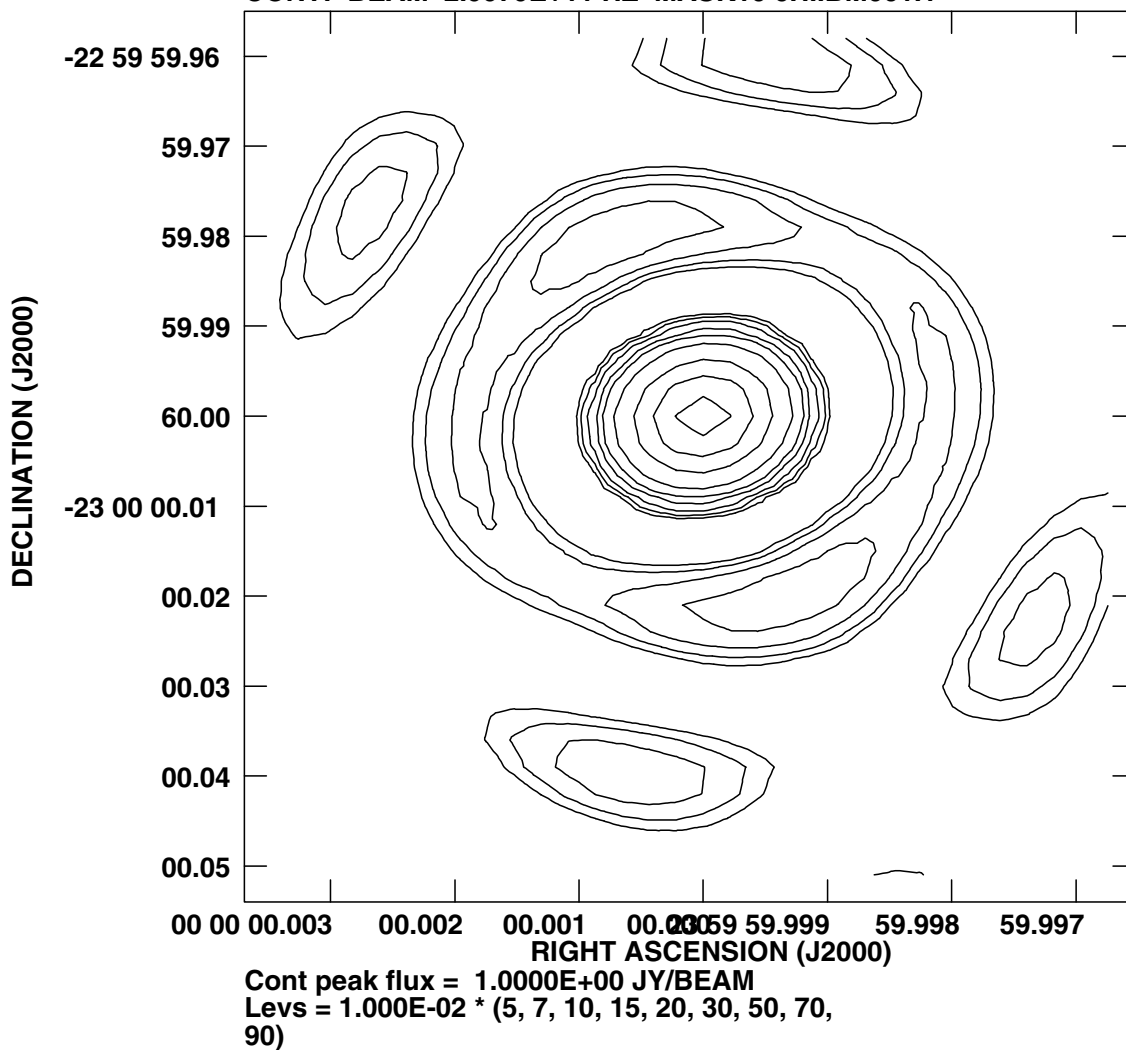


Figure 11: Six hour tracks observations. Beam pattern of the array fitted to the terrain using topography and doughnut constraints. The field (32×32 , cell = $0.2 \frac{\lambda}{D}$, $\lambda = 1mm$) includes only nearest side lobes. The side lobe level is about 17 %.

PLot file version 4 created 07-MAR-2000 10:45:16
CONT: BEAM 2.9979E+11 HZ MASK10 6H.IBM001.1

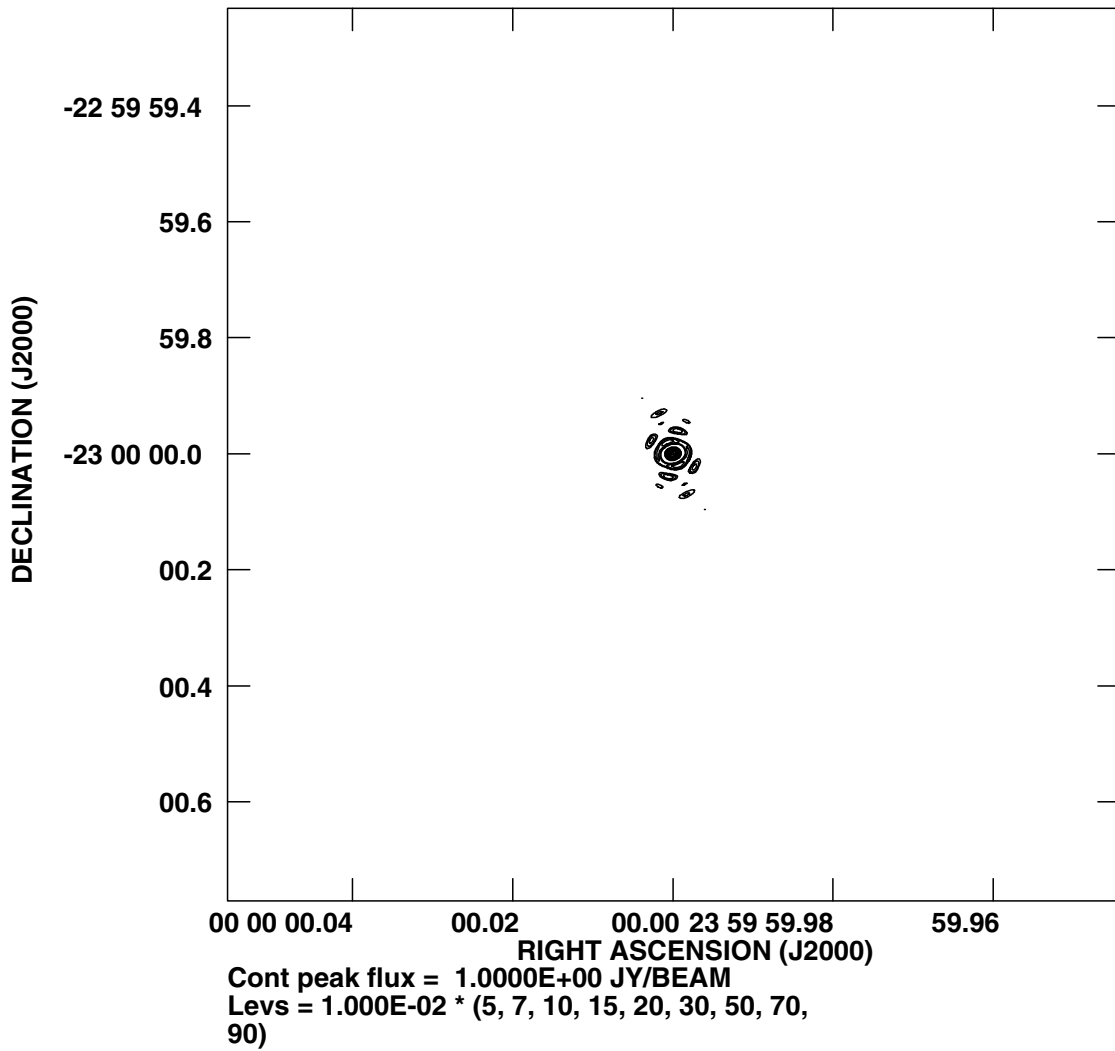


Figure 12: Six hour tracks observations. Beam pattern of the array fitted to the terrain using topography and doughnut constraints. The field (512×512 , cell = $0.2 \frac{\lambda}{D}$, $\lambda = 1mm$) includes far side lobes. The far side lobe level is less than 5 %.

PLot file version 3 created 07-MAR-2000 10:13:01
CONT: BEAM 2.9979E+11 HZ MASK7 6H.IBM001.1

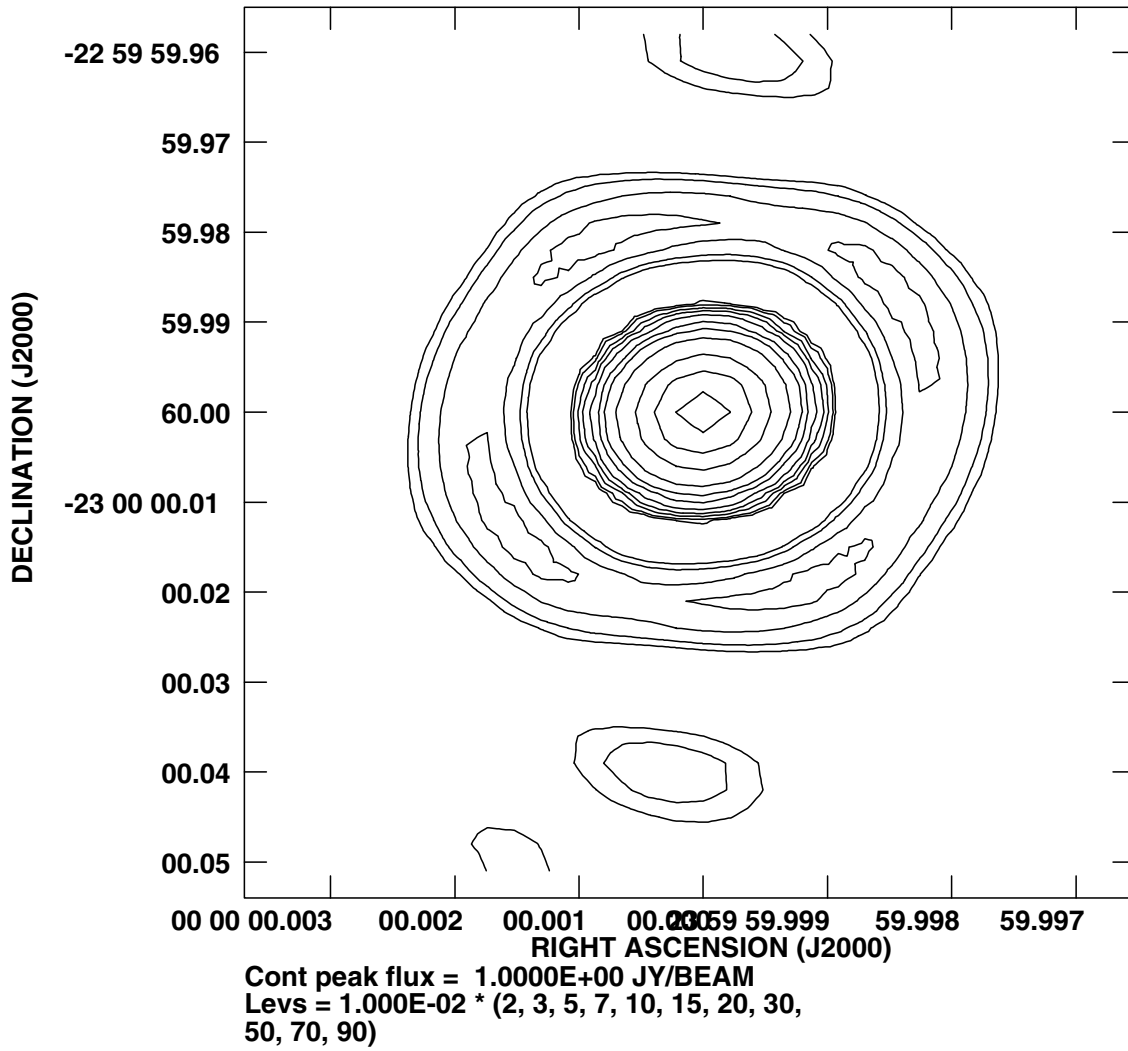


Figure 13: Six hour tracks observations. Beam pattern of the array fitted to the terrain using only topography constraints. The field (32×32 , cell = $0.2 \frac{\lambda}{D}$, $\lambda = 1mm$) includes only nearest side lobes. The side lobe level is about 8 %.

PLot file version 2 created 07-MAR-2000 10:10:36
CONT: BEAM 2.9979E+11 HZ MASK7 6H.IBM001.1

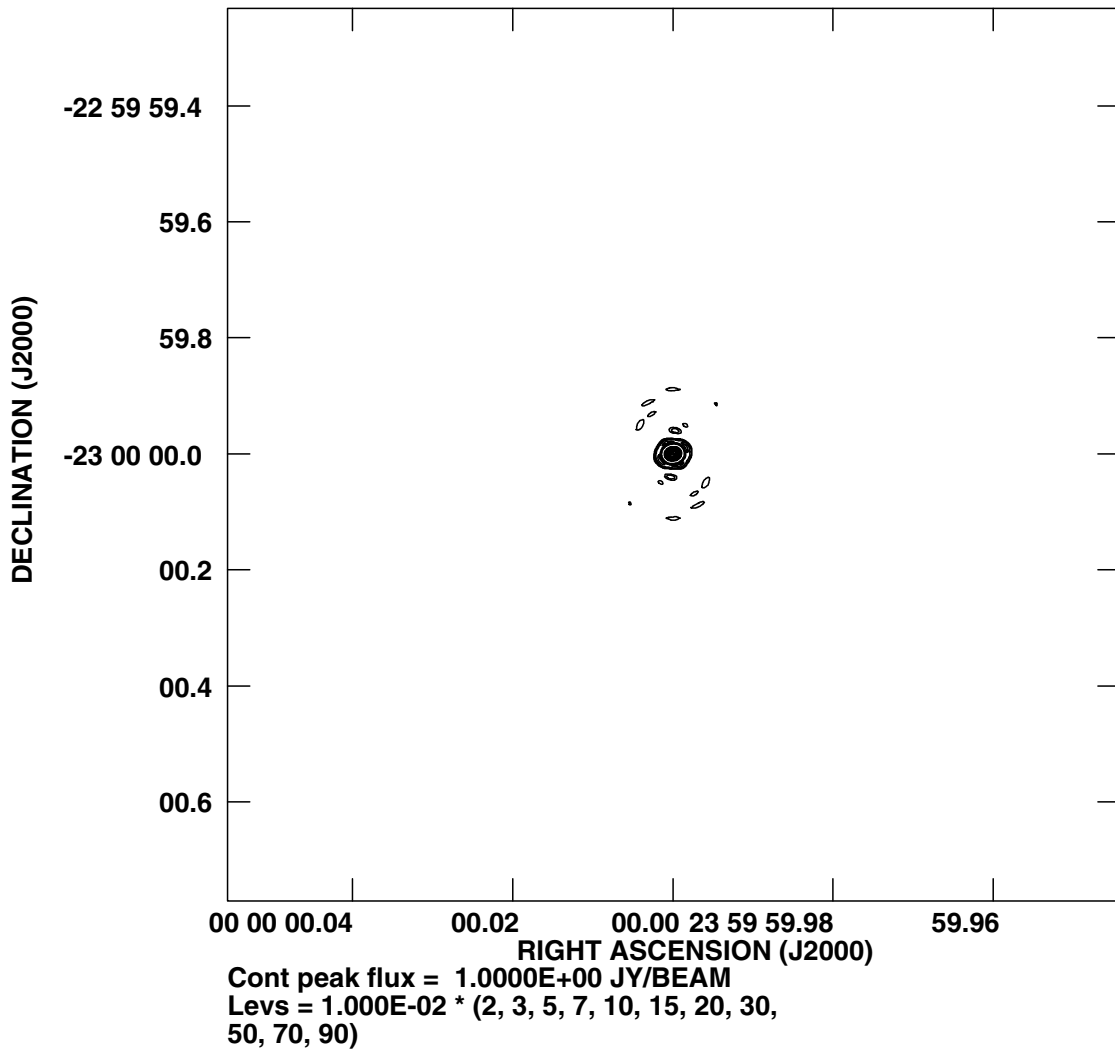


Figure 14: Six hour tracks observations. Beam pattern of the array fitted to the terrain using only topography constraints. The field (512×512 , cell = $0.2 \frac{\lambda}{D}$, $\lambda = 1mm$) includes far side lobes. UV coverage includes 6 hour tracks. The far side lobe level is less than 2 %.